PASSIVE CONTROL OF CAVITY INSTABILITIES AND NOISE

K Knowles, B Khanal, D Bray, P Geraldes
Aeromechanical Systems Group, Cranfield University
Defence Academy of the UK, Shrivenham, England. SN6 8LA

Keywords: *cavity aerodynamics, transonic flows, aeroacoustics, flow control, flow spoilers*

Abstract

Experiments and computations are presented for transonic flows over cavities having length-to-depth ratios of 4. Front and rear end walls were yawed 15° and 30°, both parallel and staggered; 3 different saw-tooth spoilers were tested on the rectangular cavity upstream lip. Cavity tones were completely eliminated with 30° yawed walls or with the largest spoiler. Hybrid RANS/LES modelling has suggested a mechanism by which the spoiler achieves tone suppression.

Nomenclature

C_p	Pressure coefficient
D	Cavity depth (m)
L	Cavity length (m)
LES	Large-eddy simulation
M_∞	Freestream Mach number
p_{rms}	Root mean square of static pressure fluctuation (Pa)
RANS	Reynolds-averaged Navier-Stokes
SPL	Sound pressure level (dB): $20 \times \log_{10}\left(p_{rms} / \left(2 \times 10^{-5}\right)\right)$
U_∞	Freestream velocity (ms^{-1})
W	Cavity width (m)
x	Streamwise coordinate from cavity upstream lip (m)
δ	Boundary layer thickness to 99% U_∞ (m)

1 Introduction

Cavity flows occur in many engineering systems from trains to aircraft. In aerospace, the most common use of cavities is in landing gear systems and weapons bays. Cavity noise is important because of its contribution to undercarriage noise, which is a major component of airframe noise. Airframe noise accounts for about half the total noise generation of a commercial aircraft during the approach; about half of the airframe noise is due to the undercarriage [1]. Cavity flow instabilities are additionally of concern in military aircraft, where they can cause problems with carriage and release of stores from internal bays [2].

Cavity flows can be defined as one of two types primarily dependent on the ratio of length to depth (L/D) of the cavity [3]. 'Open' cavity flow generally occurs in rectangular cavities with L/D<10 and is characterised by strong pressure oscillations which lead to noise radiation, structural vibration and high levels of heat transfer at the trailing edge. 'Closed' cavity flow generally occurs in cavities with L/D>13 and is regarded as a quasi-steady flow. The pressure distribution along the floor of a closed-type cavity shows a large longitudinal pressure gradient which causes a large increase in pressure drag and can lead to store release difficulties. There is generally a transitional region with 10<L/D<13 in which cavity flows exhibit a combination of open- and closed-type features. These flow category boundaries appear to be dependent on onset flow boundary layer thickness [2]. We have recently presented a detailed study of 3D, open-type cavity flows

based on PIV and pressure measurements, flow visualisation and CFD simulations [2]; we have also presented similar results for closed-type cavity flows [4] and for cavities with representative stores present [4, 5].

In this paper, new experimental results are presented for a number of passive approaches to controlling the instabilities in open-type cavity flows. These are supported by CFD calculations to gain insight into the control mechanisms being employed.

2 Experimentation

All tests were conducted using the Cranfield University, Shrivenham transonic wind tunnel. The tunnel has a working section of 206mm (height) by 229mm (width). The facility is a closed circuit, ejector-driven tunnel supplied with air from a screw-type compressor system. Dried air is supplied at up to 6 bar (gauge) to a 34m³ tank. The stored air is sufficient to run the tunnel at Mach 0.85 for about 15 seconds at a blowing pressure of 5.9 bar (gauge). The tunnel speed is maintained by varying the main inlet valve position via a feedback loop which holds a constant value of static pressure corresponding to the desired flow speed in the test section.

A rectangular cross-section cavity with L/D=4 was tested in this facility at M=0.85. The cavity (L=100mm, D=25mm, width W=60mm) was located in a flat aluminium plate (500mm long and 206mm wide) with a sharp leading edge, mounted 10mm off one side wall of the tunnel. The length of the cavity could be varied (up to a maximum of 250mm) by using rectangular filler blocks (as indicated in Fig. 1). The leading edge of the cavity was approximately 125mm downstream of the sharp leading edge of the plate. The centreline of the floor of the cavity was fitted with 0.9mm-diameter pressure tappings equally spaced every 6.25mm (giving 16 tappings along the L/D=4 cavity). These were connected to an electronically-scanned pressure transducer block (*Scanivalve ZOC22B*) via 40mm lengths of silicone tubing. The frequency response of this system was calibrated using a custom-designed rig and the resulting transfer function applied to the unsteady pressure measurements presented here.

The effect of the front and rear end walls being yawed was investigated using triangular-section insert blocks (see Fig. 1). Both parallel (Fig. 1(i)) and staggered (Fig. 1(ii)) end walls were investigated with both 15° and 30° wall yaw angles in each case; centreline length was kept constant when the end walls were yawed. For the rectangular planform baseline cavity 3 different saw-tooth spoilers (coarse, medium and fine) were tested, projecting vertically into the onset flow at the cavity upstream lip (Fig. 2). These spoilers were made of 1mm steel sheet, attached to the upstream wall of the cavity, with triangular 'teeth' projecting into the onset flow. The coarse spoiler had 8 teeth, each 3.7mm (0.15D) high by 7.4mm (0.3D) wide; the medium spoiler had 16 teeth, each 3.7mm high by 3.7mm wide; and the fine spoiler had 16 teeth, each 1.8mm (0.07D) high by 3.7mm wide.

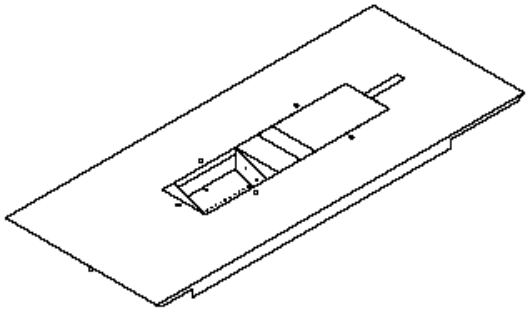

(i) Cavity with 15° slanted walls (parallel).

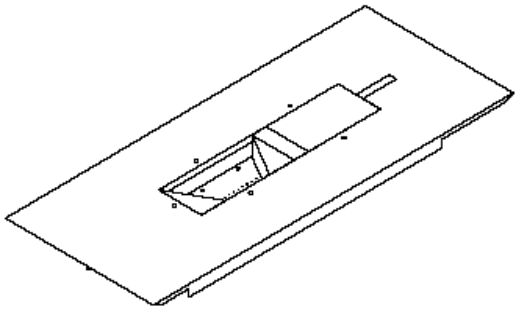

(ii) Cavity with 30° slanted walls (staggered).

Fig. 1. Yawed cavity endwall configurations:

i) parallel walls; ii) staggered walls.

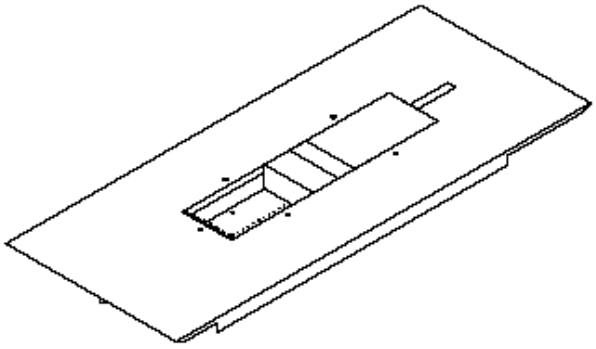

Fig. 2. Rectangular L/D=4 cavity with coarse spoiler at upstream lip.

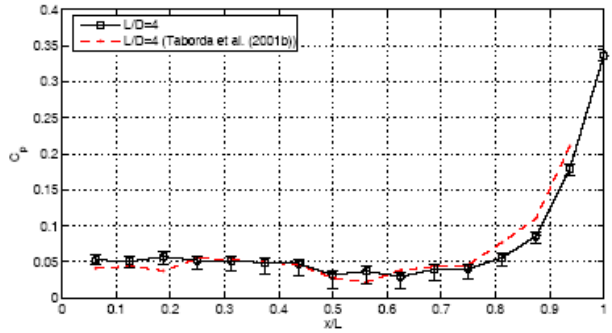

Fig. 3. Pressure coefficient distribution along the clean L/D=4 cavity centreline; comparison with experimental results of Taborda et al. [7].

3 Numerical Modelling

Two types of 3D geometries were considered. The first was a three-dimensional plane cavity, which comprised a simple rectangular cutout in an otherwise infinite plate and is therefore fully described by its length-to-depth and length-to-width ratios. The second type had a spoiler at the upstream edge, similar to the coarse spoiler in the experiments. The three-dimensional computational domains extended 4L upstream, 5L downstream and 3L vertically and laterally from the cavity. The overall mesh size for all the cases was maintained approximately between 1.9 million cells and 2.5 million cells. Grid cells were clustered along all solid walls and in the region of the shear layer using a hyperbolic-tangent distribution. At the cavity leading edge, the boundary layer is resolved with approximately 20 mesh points and was set to match the measured δ. The CFD solver FLUENT was used with a hybrid RANS/LES turbulence model (DES). Further details of the numerical modelling are given by Khanal et al. [6].

4 Results and Discussion

The mean pressure distribution along the centreline of the rectangular cavity floor (Fig. 3) was seen to be typical of open-type cavity flows, as discussed by Plentovich et al. [3]. The distribution was also in close agreement with earlier measurements by Taborda using the same rig [7].

The unsteady pressure fluctuation levels in the rectangular cavity are presented in Figure 4 for the tapping at x/L=0.94. The frequencies of the first three tones are compared with theoretical predictions using the modified Rossiter equation (see [2]). Also shown is the pressure fluctuation spectrum for a flat plate in the tunnel. The flat plate unsteady pressure levels were measured using the cavity floor plate mounted so that the surface with the static pressure tappings was flush with the main flat plate. The pressure readings were measured in the same way as the cavity floor pressure fluctuations. The pressure data obtained consisted of 700 samples per transducer, sampled at 16.6 kHz obtaining the pressure history for 30 transducers (covering approximately twice the streamwise length of the L/D=4 cavity). The data from each of the pressure transducers were treated using an FFT in order to extract the spectral pressure variation. The results from the spectral analysis were very similar for all the tappings and the spectra for all 30 pressure tappings were averaged into one. Thus, Figure 4 shows the increase in broadband pressure fluctuation levels caused by the cavity, as well as the tones that are generated.

Three tones are visible in Figure 4, with the first tone clearly having the highest amplitude. This first-mode dominance was also seen for all the tappings along the cavity floor, as shown in Figure 5. Also shown in Figure 4 are the tone frequencies predicted by the modified Rossiter equation [2], with a 2% tolerance.

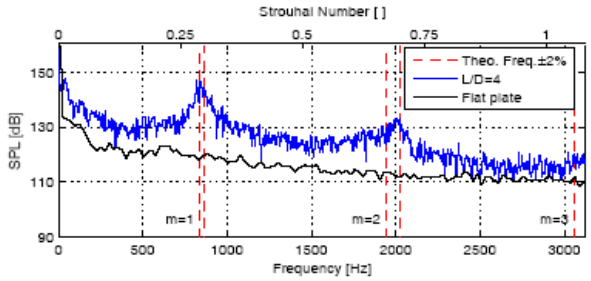

Fig. 4. Frequency spectrum of the clean L/D=4 cavity compared with the empty wind tunnel section.

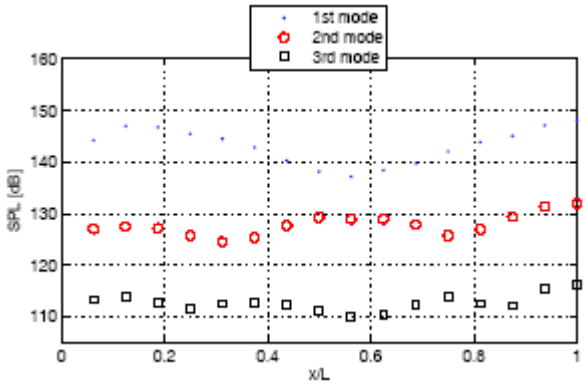

Fig. 5. Streamwise variation of tone amplitudes along the centreline of the clean L/D=4 cavity

4.1 Effects of Yawed End-walls

We now consider various passive approaches for reducing the amplitudes of the cavity tones discussed above. Figures 6 to 9 show the effects of non-rectangular planforms, in terms of cavity spectra near the downstream wall. With only 15^o of end-wall yaw there is very little reduction in the tone levels: the staggered configuration (Fig. 6) being slightly better than the parallel one (Fig. 7). With 30^o of end-wall yaw, on the other hand, there is a dramatic reduction in tone levels. The staggered configuration (Fig. 8) is again more effective than the parallel one (Fig. 9). Although the parallel configuration causes a reduction in tone levels the residual tones are also shifted somewhat in frequency. The large reduction in tone levels caused by the 30^o staggered wall configuration is emphasized by comparing the streamwise variation of tone levels in Figure 10 with the baseline case in Figure 5.

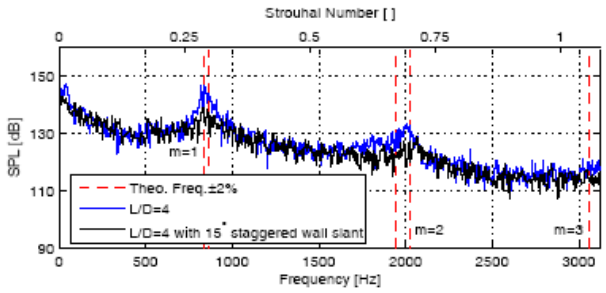

Fig. 6. Cavity spectra with and without 15o wall yaw (staggered walls).

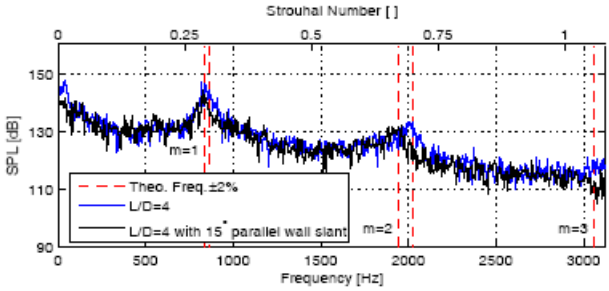

Fig. 7. Cavity spectra with and without 15^o wall yaw (parallel walls).

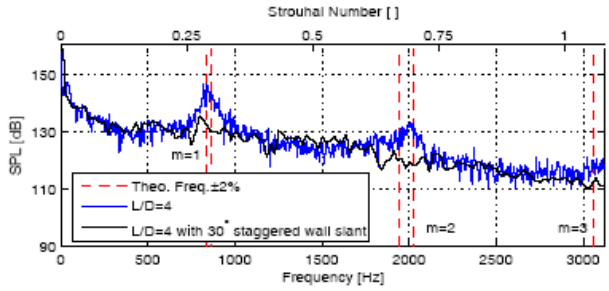

Fig. 8. Cavity spectra with and without 30^o wall yaw (staggered walls).

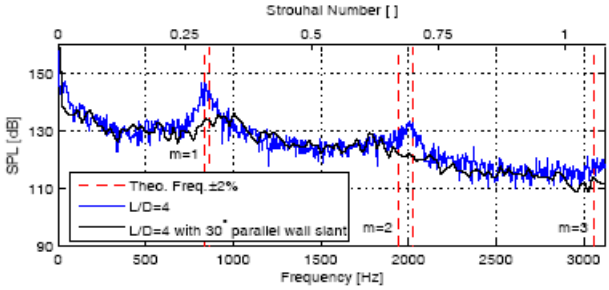

Fig. 9. Cavity spectra with and without 30^o wall yaw (parallel walls).

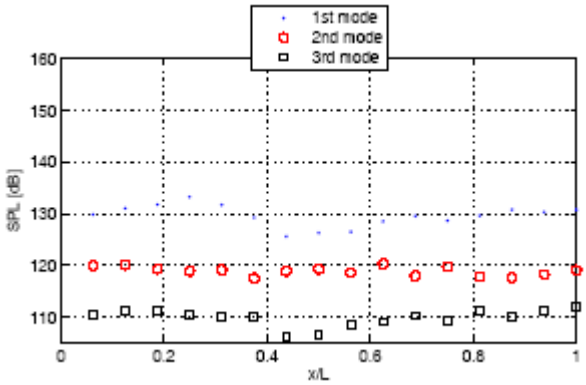

Fig. 10. Streamwise variation of tone amplitudes along the centreline of the cavity with walls yawed at 30° (staggered walls).

4.2 Effects of Saw-tooth Spoilers

The results obtained from the use of saw-tooth spoilers as a means of reducing the tones produced by the L/D=4 cavity at M_∞=0.85 are now considered. The objective of the spoilers was to introduce disturbances into the shear layer in order to disrupt the resonant mechanism that sustains the cavity oscillations [8].

Figures 11 to 13 show the resulting spectra from the application of an FFT to the pressure signal measured at 0.9375L with and without a spoiler. These figures serve as comparison of the tone attenuation achieved by the different scales of perturbation induced on the shear layer. Figure 11 shows that the large spoiler effectively attenuates the cavity resonant frequencies since the spectrum measured for this configuration is reduced to broadband noise. The spectra in Figure 12 show the result of the application of the medium spoiler. In this case there is still a complete attenuation of the second resonant mode and although there is a significant reduction in the first mode, the effect of this spoiler on the first mode is not as great as the large spoiler.

The spectra in Figure 13 show the results of the application of the small spoiler. In this case there is still an attenuation of the resonant modes, however this attenuation is not as high as for the other spoilers. The small spoiler still induces a reduction in SPL for the first mode frequency, although the effect of this spoiler on the second mode is not as noticeable as with the previous cases.

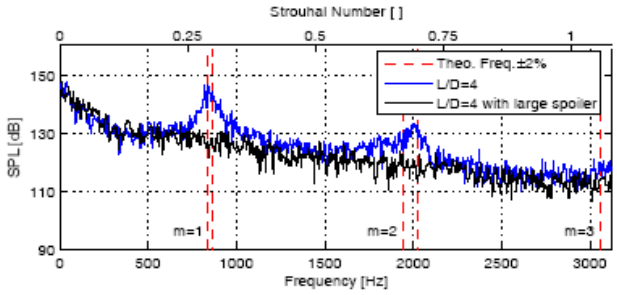

Fig. 11. Frequency spectra near downstream wall for the cavity with coarse (large) spoiler and the clean cavity.

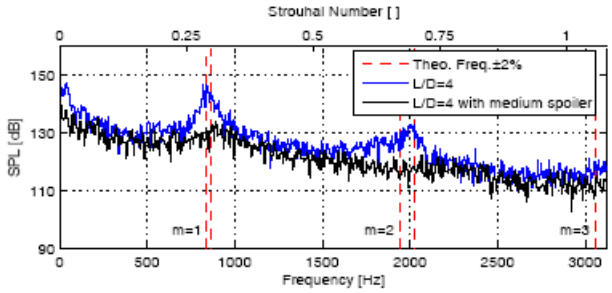

Fig. 12. Frequency spectra near downstream wall for the cavity with medium spoiler and the clean cavity.

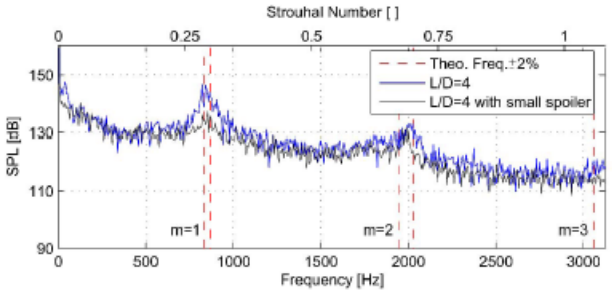

Fig. 13. Frequency spectra near downstream wall for the cavity with fine (small) spoiler and the clean cavity.

To put the spoiler performance in context the onset flow boundary layer needs to be considered. This was measured with a Pitot probe located 10mm upstream of the cavity leading edge. Mean boundary layer thickness

was found to be δ=17.3mm (δ=0.7D). This comparatively thick boundary layer was found to be the result of flow separation at the leading edge of the flat plate and downstream reattachment. The large spoiler thus has teeth which are 0.21δ high. Increasing the number of teeth (and, therefore, the number of streamwise vortices generated) with the medium spoiler, by reducing their width (from 0.43δ to 0.21δ), only slightly reduces the spoiler's effectiveness. On the other hand, reducing the height of the teeth to only 0.1δ dramatically reduces the spoiler's effectiveness.

4.2.1 Results of numerical modelling

The numerical modelling of the clean cavity and the cavity with the coarse spoiler has provided detailed flowfield data that were not available from the experiments alone. As discussed by Khanal et al. [6], the predicted clean cavity mean pressure distribution matched that presented in Figure 3, whilst the unsteady pressure distribution also showed good agreement with the coarse-spoiler spectrum of Figure 11. The predicted clean cavity spectrum, however, showed second mode dominance, unlike the experiments (Fig. 4), with a lower frequency for the second mode than seen experimentally or predicted by the modified Rossiter equation. Reasons for this discrepancy are discussed by Khanal et al. [6]. Overall, however, the agreement between the computations and the experiments was sufficiently close as to give confidence in deductions drawn from the former.

Visualisation of the free shear layer over the cavity (Fig. 14) shows a marked increase in the organization of flow structures in the case with the spoiler. Strong streamwise vortices are generated by the teeth of the spoiler. Unsteady visualization of the flow evolution, for the clean cavity, shows 'warping' across the width of the cavity of flow structures as they progress downstream. By contrast the spoiler seems to impede this warping. Khanal et al. [6] discuss this in more detail and how it reduces the unsteady pressure levels in the cavity.

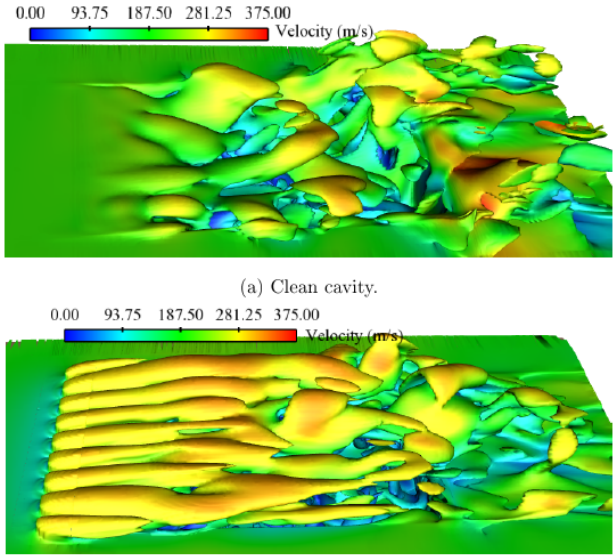

Fig. 14. Vorticity iso-surfaces, coloured by velocity, showing flow structures in the shear layer; L/D=4, W/D=2.4, M_∞ = 0.85; (a) clean cavity and (b) cavity with coarse spoiler.

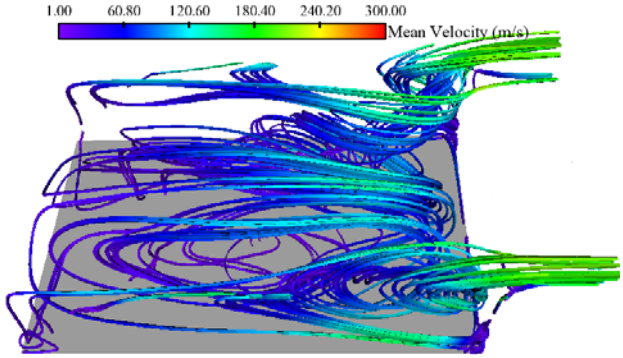

Fig. 15. Stream traces coloured by speed for a clean cavity flow; L/D=4, W/D=2.4, M_∞ = 0.85; upstream and side walls removed for clarity

The mean flow is also seen to be dramatically altered by the spoiler. Figure 15 shows stream traces inside the clean cavity. This reveals 'tornado-like' vortices either side of the centre-line in the upstream quarter of the cavity (as discussed by Atvars et al. [2]). These spiral up towards the free shear layer before being swept downstream into the primary recirculation zone inside the cavity. Also seen in Figure 15 are the two streamwise vortices that are shed

from the downstream corners of the cavity. These stem from the primary recirculation zone, as emphasized in Figure16. The effect of the coarse spoiler is seen in Figures 17 and 18. It is immediately apparent that the mean flow is much more uniformly distributed across the span, inside the cavity as well as in the shear layer, and that corner vortices are no longer prominent features. The main feature of the mean flow pattern on the cavity floor is also consistent with the oil flow visualization of Geraldes [8] who observed a separation line at x/L = 0.25 to 0.3, towards which all the streamlines converge. In the CFD the streamlines are seen to converge at approximately x/L = 0.3.

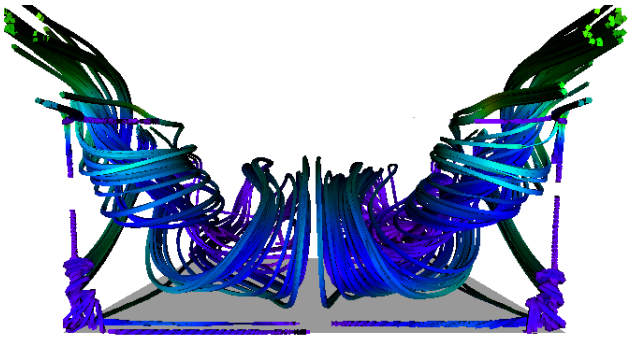

Fig. 16. Stream traces for a clean cavity flow; L/D=4, W/D=2.4, $M_\infty = 0.85$; viewed from the downstream end-wall looking upstream - end and side walls removed for clarity

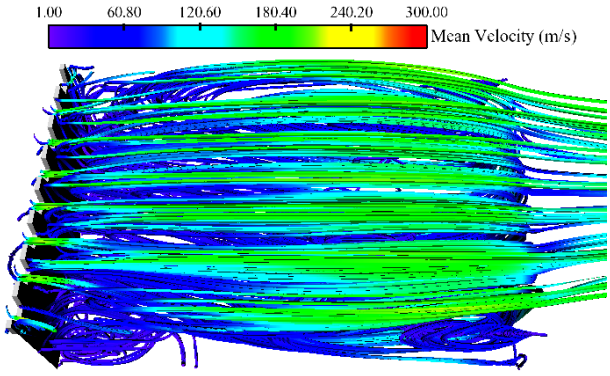

Fig 17 Stream traces coloured by speed for a cavity flow with coarse spoiler; L/D=4, W/D=2.4, $M_\infty = 0.85$; cavity walls removed for clarity

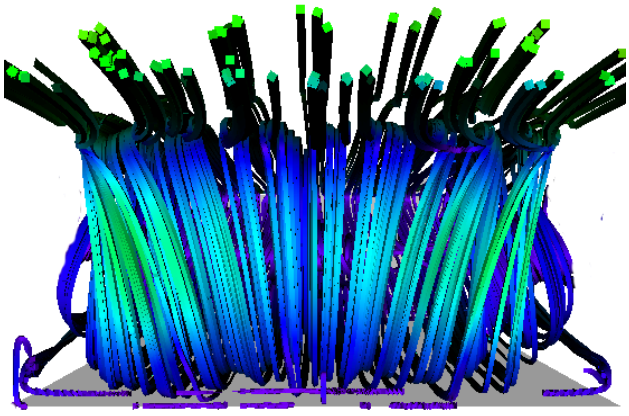

Fig 18 Stream traces for a cavity flow with coarse spoiler; L/D=4, W/D=2.4, $M_\infty = 0.85$; viewed from the downstream end-wall looking upstream - end and side walls removed for clarity

To try to understand the mechanism by which the spoilers reduce cavity resonance, the unsteady flowfield was examined by visualising its time-evolution. The computed flow inside the cavity was found to be highly unsteady and dominated by periodic phenomena. Tubular vortical structures inside the cavity were seen to affect the shear layer, but overall the shear layer spanning the cavity width is found to be more stable in the case with the spoiler. To explain this, first the origin of spanwise fluctuations in a 3D clean cavity needs to be explained. The shear layer above clean cavities undergoes a warping across the cavity width, which is partly due to the slowing down of the flow by the side walls. But the main reason can be described as follows.

The wall shear stress due to the three-dimensional flat-plate boundary layer upstream of the leading edge of a 3D cavity results in a component of viscous force in the spanwise direction. When the flow separates at the cavity leading edge, this spanwise force acts as an initial trigger for the spanwise oscillation of the separated shear layer. The oscillation gets energized by the presence of unsteady turbulent energy in the flow. In the case of a spoiler, however, the spoiler and its strong streamwise vortices act as a barrier against the spanwise instability. In addition, the loss of turbulent kinetic energy due to the presence of the spoiler

means the shear layer instabilities do not get enough energy to amplify. This is thought to be the reason for the stable separated shear layer.

Tubular structures within the cavity are seen to arrive at the cavity leading edge but these structures do not have sufficient energy to cause the violent flapping of the streaks of the separated shear layer. Therefore the sustained fluctuation of the shear layer does not occur. In other words, the resonant modes are absent.

5 Conclusions

Experiments have been reported on an L/D=4 cavity at M_∞=0.85 to investigate potential passive solutions to open-cavity flow resonance. Two categories of device were tested: yawed cavity end-walls; and leading-edge spoilers. 15° and 30° of end-wall yaw were investigated, with both parallel and staggered configurations. Staggered end-walls were found to be more effective than parallel ones, and 30° of yaw was found to be better than 15°. Thus, the 30° staggered configuration almost entirely suppressed the cavity tones, whereas the 15° parallel configuration had negligible effect on the tones.

Three different serrated spoilers were tested at the cavity leading edge. An 8-tooth spoiler which projected 0.15D (0.21δ) into the onset flow was found to eliminate the cavity tones completely. Doubling the number of teeth slightly reduced the effectiveness of the spoiler, but additionally halving its height (to 0.1δ) completely destroyed its efficacy.

Numerical modelling of the cavity flow with the coarse spoiler has been conducted using a hybrid RANS/LES scheme. Based on results from these calculations a mechanism has been postulated by which the spoiler removes the cavity resonance. It is seen that the spoiler generates strong streamwise vortices which absorb turbulent energy from the approaching boundary layer and resist the cross-stream warping of transverse vortical structures in the free shear layer. Unsteady flow within the cavity has insufficient energy to excite flapping of this free shear layer.

References

[1] Anon. *Science & Vie* - Hors Série, Aviation 2001, nº 215 Juin 2001

[2] K. Atvars, K. Knowles, S.A. Ritchie and N.J. Lawson. Experimental and computational investigation of an "open" transonic cavity flow. *Proc IMechE, Pt G: J Aerospace Engineering*, Vol. 223, No. G4, pp 357-368, 2009.

[3] E.B. Plentovich, R.L. Stallings and M.B. Tracy. Experimental cavity pressure measurements at subsonic and transonic speeds. *NASA TP-3358*, 1993.

[4] K. Knowles, S.A. Ritchie and N.J. Lawson. An investigation of the flow in a 3D, shallow transonic cavity with and without representative stores. *Proc 7th Int ERCOFTAC Symposium on Engineering Turbulence Modelling and Measurements - ETMM7.* Limassol, Cyprus. 4 - 6 June 2008.

[5] K. Knowles, N.J. Lawson, D. Bray, S.A. Ritchie and P. Geraldes. Studies of transonic cavity flows relevant to aircraft stores carriage and release. *Proc NATO RTO Meeting AVT 108 - Weapons Integration with Land and Air Vehicles*. Williamsburg, USA. 7-10 June 2004.

[6] B. Khanal, K. Knowles and A.J. Saddington. Computational investigation of cavity flow control using a passive device. *Proc Royal Aeronautical Society Aerodynamics Conference 2010 - Applied Aerodynamics: Capabilities and Future Requirements*. Bristol, UK. 27-28 July 2010.

[7] N. Taborda, D. Bray, and K. Knowles. Passive control of cavity resonances in tandem configurations. *Proc 31st AIAA Fluid Dynamics Conference*. Anaheim, CA, USA. 11-14 June 2001. Paper No AIAA-2001-2770.

[8] P Geraldes. Instabilities in transonic cavity flows. *PhD thesis*, Cranfield University (Shrivenham). October 2005.

Contact Author Email Address

The contact author is Prof K Knowles:

K.Knowles@cranfield.ac.uk

Copyright Statement